

Single ionization of He by low-velocity protons and C^{6+} : Ejected electron momentum distributions

S. D. Kravis, M. Abdallah, C. L. Cocke, C. D. Lin, M. Stockli, B. Walch, and Y. D. Wang
J. R. Macdonald Laboratory, Department of Physics, Kansas State University, Manhattan, Kansas 66506

R. E. Olson
Laboratory for Atomic and Molecular Research and Physics Department, University of Missouri–Rolla, Rolla, Missouri 65439

V. D. Rodríguez
Departamento de Física, Universidad de Buenos Aires, 1428 Buenos Aires, Argentina

W. Wu and M. Pieksma
Oak Ridge National Laboratory, Oak Ridge, Tennessee 37831

N. Watanabe
The Institute of Physical and Chemical Research (RIKEN), Wako, Saitama 351-01, Japan
(Received 31 January 1996)

A technique for electron spectroscopy which yields full two-dimensional momentum distributions for continuum electrons has been used to study ejected electrons from single ionization of He by C^{6+} and proton projectiles at low velocities. Projectile velocities of 1.63, 1.38, and 1.16 a.u. for C^{6+} and 2.39, 1.71, 1.15, .85, and 0.63 a.u. for protons were used. All spectra show much broader distributions along the beam than transverse to the beam. For the case of proton bombardment, the spectra are strongly influenced by both target and projectile potentials, maximizing near the velocity of the saddle in the potential between the two receding ion cores for the lowest projectile velocities. For C^{6+} projectiles, the spectra appear to be dominated by the projectile potential and the center of the distribution is strongly shifted toward the projectile velocity. Theoretical results from the continuum-distorted-wave–eikonal-initial-state and classical-trajectory–Monte Carlo methods are in rather good agreement with the proton data but do not agree well with the C^{6+} data. [S1050-2947(96)01408-4]

PACS number(s): 34.50.Fa, 39.30.+w

I. INTRODUCTION

The ionization of a neutral target by a fast projectile of charge Z and velocity v is rather well understood if Z/v is small. (Throughout this paper we use the term “ionization” to mean that an electron is removed from the target to the continuum with no change in the projectile charge state.) Under such conditions, the process can be treated perturbatively and is dominated by “direct ionization” (DI) of electrons into the low-energy target-centered continuum. The corresponding “soft electrons” dominate the continuum electron spectrum, but there appear also in this spectrum two other prominent features associated with specific mechanisms, namely “binary encounter electrons” resulting from hard projectile-electron encounters and “cusp electrons” from electron capture to the continuum (ECC). The former follow binary encounter kinematics appropriate to projectile-free-electron encounters, while the latter are found centered on the projectile in final velocity space. For large Z and/or small v , ionization can no longer be treated perturbatively, the description of the electron spectrum in terms of soft, cusp, and binary encounter electrons ceases to be useful, and new identifications of features in the spectrum and the associated ionization mechanisms are called for. For the case of proton impact there exists extensive literature ([1] and refer-

ences therein) in both experiment and theory. Nevertheless, there remains controversy over the mechanism(s) responsible for ionization at small v . In order to address this problem, we report in this paper comprehensive experimental electron spectra for ionization of He in the nonperturbative region for both protons and C^{6+} projectiles at low v .

For intermediate- to low-velocity impact ionization, cross sections were calculated by Shakeshaft [2] for $p+H$ collisions. He found that the projectile-centered contribution to the total ionization cross section was larger than the target-centered one for impact energies below 60 keV, a surprising result, since at higher impact energies the projectile-centered contribution is only a small fraction of the total ionization cross section. A possible explanation for the relative increase of ECC is that electron capture becomes increasingly important relative to the DI process as the collision velocity is lowered, and eventually completely dominates the collision dynamics. Also, in the low-energy region the calculated cross sections were well below the measurements by Park *et al.* [3]. Performing classical-trajectory–Monte Carlo (CTMC) calculations on $p+H$ collisions with impact energies from 25 to 200 keV, Olson [4], found that a significant number of continuum electrons had velocities near $v_p/2$, where v_p is the velocity of the projectile. He attributed these electrons to target ionization that could occur by stranding

continuum electrons on the saddle of the potential between the two receding Coulomb centers. Experimentally, these $v_p/2$ electrons were later measured by Olson *et al.* [5]. Winter and Lin [6] used a triple-center atomic-state method, where the third center was at the unstable equilibrium point (saddle point in the potential) between the nuclei for $p+H$ collisions having impact energies between 1.5 and 15 keV. At these low-impact energies they found that the bound states localized on the third center were the primary ionization channels. This triple-center method explicitly takes into account electrons originating from the saddle point in the potential. A classical description of this mechanism would be the following. As an ion approaches an atom, the potential wells separating them lowers enough that the electron from the atom can overcome its parent potential barrier, becoming “molecular.” If the electron resides on top of the potential barrier (saddle point) as the two centers separate, the electron gets “pushed up” as the potential barrier increases and the electron is finally ionized when the collision partners are far apart. In an alternative adiabatic potential-energy curve description of this process [7], the electron is promoted diabatically through a series of crossings [8], which track the top of the potential barrier as the centers separate, finally ending up in the continuum. A continuum electron so generated will have a velocity near the velocity of the saddle point, which is given by

$$v_s = \frac{v_p}{1 + q_p^{1/2}/q_t^{1/2}}, \quad (1)$$

where v_p is the velocity of the projectile and q_t and q_p are the charge states of the target and projectile (respectively) after ionization. In the curve-crossing treatments discussed by several authors [7–10], this process is referred to as the T process.

Many experimental and theoretical searches for these saddle-point electrons have been made, and the subject continues to generate controversy. Evidence for saddle-point electrons was found experimentally by Irby *et al.* [11] in H^+ and He^{2+} collisions with He, Ne, and Ar. More recent results by DuBois [12] disagree with the results from Ref. [11], claiming that the T process is not important. Recent results by Irby *et al.* [13] using C^+ , C^{2+} , and C^{3+} projectiles on He and Ne targets also exhibited evidence for the saddle-point mechanism. Again, these conflict with results from DuBois [14] using C^0 , C^+ , C^{2+} , C^{3+} , and C^{4+} on He. Furthermore in Ref. [14], it is concluded that using “dressed” (not fully stripped) projectiles is inappropriate when searching for saddle-point electrons. This is due to direct projectile-electron–target-electron interactions, which increases the cross section for low-energy electron emission from the target beyond that of a bare projectile of the same charge state. Meckbach *et al.* [15] also dispute the existence of saddle-point electrons based on their experimental results for $p+He$ at 52- and 103-keV collision energies. Pieksma *et al.* [16] pointed out that the T process can be described in terms of adiabatic theories that are applicable to collision velocities less than 1 a.u., well below the velocity range of the above-mentioned experiments. Pieksma *et al.* measured the ejected

electron velocity distributions in $H^+ + H$ collisions at energies between 1 and 6 keV and interpreted their results as evidence for the T process.

A second mechanism for low-energy ionization is the S process discussed by [9]. In the S process ionization occurs as the two nuclei approach each other at small internuclear distances, where the target electron can be diabatically promoted into the continuum through a series of hidden crossings [7]. A classical description of the process might be that, as the two nuclei approach very close to each other, a centrifugal barrier is formed that forbids the electron from existing between the two nuclei. An electron “riding” on this barrier will be diabatically pushed up as the nuclei approach each other and left in an excited or continuum state. Recent theoretical results by Ovchinnikov and Macek [10] for proton impact on H with a velocity of 0.4 a.u. show that S -type electrons are peaked in momentum space at both the target and projectile. When considering the S and T processes in the hidden-crossing framework, these processes are clearly molecular in nature and thus this description is best suited to low-impact velocities, where molecular effects are important.

For highly charged naked ion impact on He, Wu *et al.* [17] investigated ionization at low velocities ranging from 0.2 to 1.7 a.u. for C^{6+} , N^{7+} , O^{8+} . Data were also presented for the dressed ions Ar^{16+} and Xe^{30+} . From the total-ionization cross sections determined from the experiment, they found a scaling relation similar in form to that expected for saddle-point ionization. Though not conclusive evidence, the agreement between the experimental and theoretical scaling relation is consistent with the hypothesis that the saddle-point mechanism is important in these collisions in the scaled velocity range of $0.7 \leq v_p q_p^{-1/4} \leq 1.03$ a.u. However, identification of the ionization mechanism from total cross sections alone is at best very risky, and we were thus led to seek a more definitive feature of the mechanism by measuring the momentum-space distributions of the continuum electrons. For the S and T processes, these distributions are expected to be quite different. T -process electrons should lie near v_s , while S -process electrons should be centered near the projectile and target (for symmetric collisions) and near the center of mass for highly charged projectiles [7].

In this paper we present experimental and theoretical results for the ejected electron momentum distributions (EEMDs) in two dimensions (integrated over the third momentum component) for single ionization in collisions of protons and C^{6+} on He. The EEMD parallel (Z) to the projectile beam axis and one-component perpendicular (Y) to the beam axis were measured. We use a technique for electron spectroscopy that gives a complete two-dimensional view of the electron momentum distribution as opposed to the usual measurement of electron-energy spectra at selected angles. This technique results in a two-dimensional image that qualitatively gives a clear picture of the ejected electron angular distribution. One-dimensional projections of the two-dimensional distributions yield quantitative spectra that can be compared with definite theoretical predictions. For the proton data the projectile velocities were $v_p = 2.39, 1.71, 1.15, 0.85,$ and 0.63 a.u. corresponding to projectile energies of 143, 73, 33, 18, and 10 keV. The projectile velocities for the C^{6+} data were $v_p = 1.63, 1.38,$ and 1.16 a.u. corresponding to 858, 618, and 438 keV projectile energies. The use of

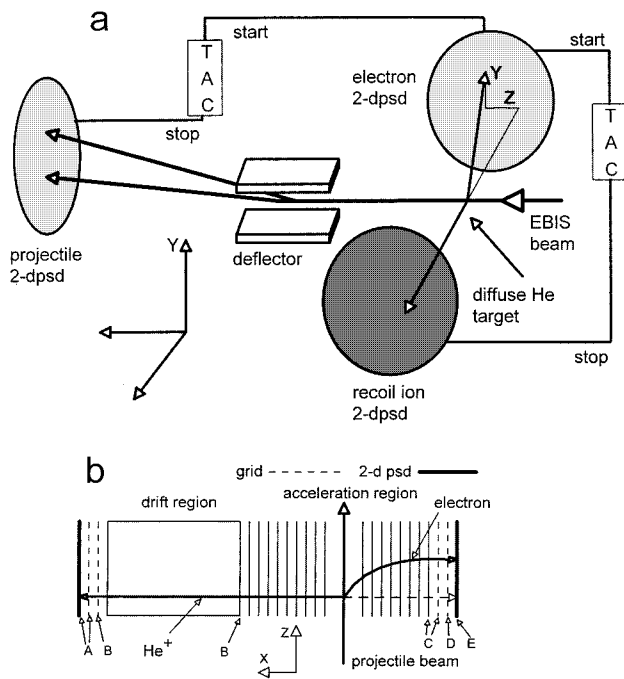


FIG. 1. Schematic of the experimental setup illustrating the geometry of the three two-dimensional position sensitive detectors (2-dpsd) for triple coincidence between the ejected electrons, recoil ions, and projectiles. Also included is a schematic of the time-of-flight spectrometer (b). The plates in the acceleration region are connected together by a resistor chain so that a uniform field is created. The letters correspond to the following applied potentials: $A = -3.02$, $B = -3.03$, $C = 0.50$, $D = 0.25$, and $E = 0.21$ kV.

naked C^{6+} ions precludes any contributions to the ionization cross section by direct projectile-electron-target-electron interactions, thus resulting in less ambiguity in the interpretation of the spectra, addressing the problems related to the dressed-projectile-target ionization mentioned in Ref. [14].

Two theoretical treatments are used here. One is the continuum-distorted-wave-eikonal-initial-state (CDW-EIS) method [18,19] and the other is the classical-trajectory-Monte Carlo (CTMC) method [20]. Application of the CDW-EIS method to the present experiment has been given in detail in Ref. [21]. The CDW-EIS model has the important feature that the ejected electron is described as moving in the combined field from both the target and the projectile ions. Since the CDW-EIS model includes effects due to the long-range nature of the target and the projectile interactions in the entrance and exit channels, it has proven to be quite successful in describing ionization of atoms by protons and by other heavy ions at high to intermediate impact energies.

II. EXPERIMENTAL TECHNIQUE

The experiment was carried out in the J. R. Macdonald Laboratory at Kansas State University. The protons and C^{6+} ions were provided by the KSU CRYEBIS facility [22]. Figure 1(a) illustrates the experimental setup and Fig. 1(b) is the time-of-flight (TOF) spectrometer that was used to detect the

recoil He ions and ejected electrons. The TOF spectrometer's axis was positioned perpendicular to the projectile beam that passed through a spectrometer region of uniform electric field of 420 V/cm. This uniform electric-field region extended 3.8 cm toward the direction of increasing positive potential where a two-dimensional position-sensitive detector (2-dpsd) was positioned for detecting electrons. The He^{q+} recoil ions were accelerated in the opposite direction through 4.5 cm and then entered a field-free drift region of 7.1 cm after which they were detected by another 2-dpsd. The electron and recoil ion detectors were identical, using microchannel plates in a chevron configuration with a wedge-and-strip-type anode. The magnetic field in the spectrometer region was kept below 50 mG by three sets of Helmholtz coils oriented perpendicular to each other. After exiting the spectrometer, the projectile beam passed through an electrostatic deflector that separated the projectile charge states and then was detected by another 2-dpsd. The C^{6+} projectiles, He^{q+} recoil ions, and ejected electrons were detected in a triple coincidence mode as indicated in Fig. 1(a). This allowed us to separate unambiguously the low-cross-section ionization channel from the larger single-capture, double-capture, and transfer ionization channels. For example, our spectra for the ionization channel were gated on the projectile detector position corresponding to C^{6+} , the He^+ time peak in the recoil-electron TOF spectra, and the time peak in the electron-projectile TOF spectra. The last gate was necessary to reduce a subtle background from the reaction $C^{6+} + He \rightarrow C^{5+} + He^+ + h\nu$, where the photon was detected by the electron detector and the C^{5+} ion was not detected. In this situation it is possible to register a C^{6+} from the intense main beam within the strobe time ($\approx 5 \mu\text{sec}$) of the data acquisition computer, but less likely for it to occur during the 0.02- μsec -wide electron-projectile time-to-amplitude converter (TAC) peak. The count rate on the projectile detector ranged from 30 to 100 kHz. For the proton data, only coincidences between the He^+ recoils and electrons were necessary. A diffuse He gas target was used in the vacuum chamber housing the spectrometer and the target pressure was kept below 5×10^{-6} Torr, making double collisions improbable. Contamination of the C^{6+} beam with C^{5+} was less than 1%.

The electron momentum was determined in the following way. The He recoils is born with low energy, is quickly accelerated in the high-electric-field region of the spectrometer, and travels in a nearly straight line trajectory to the recoil detector, pinpointing the origin of the ionization event. The electron is accelerated in the opposite direction and its position on the detector is recorded. The recoil (Y, Z) position (origin of the electron) is subtracted from the electron (Y, Z) position that results in a (Y, Z) position spectrum proportional to the initial Y and Z components of the electron momentum (see Fig. 1). The proportionality constant between the position and momentum can be calculated using the known dimensions and electric fields in the spectrometer. Verification of the calculated constant was accomplished by examination of the $3l3l'$ transfer ionization channel in the present $C^{6+} + He$ data. The resulting Auger lines following double capture into the $3lnl'$ states have been measured by Stolterfoht *et al.* [23] and the energy levels of these states have been calculated by Bhalla *et al.* [24]. This channel can

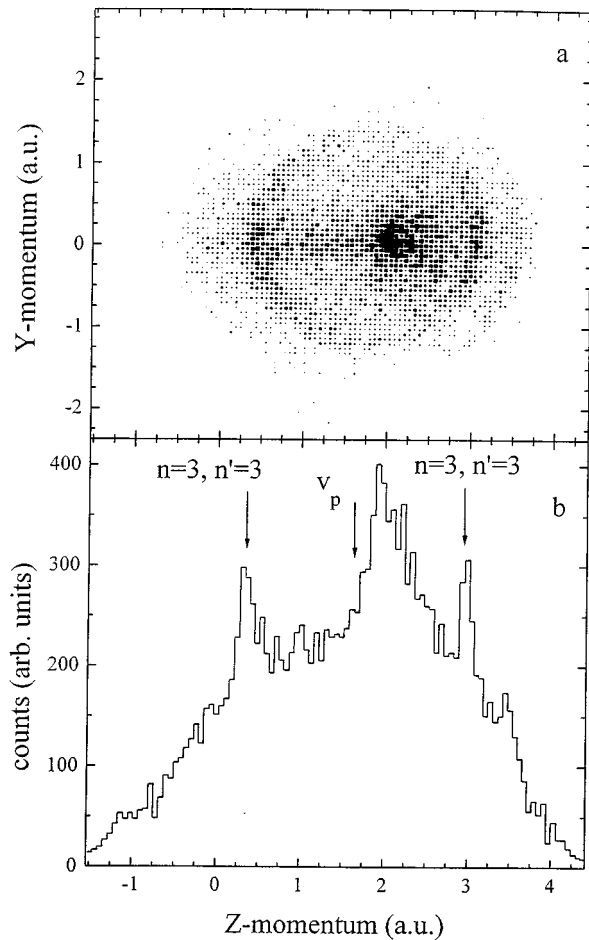


FIG. 2. Two-dimensional electron momentum distribution (a), from the transfer ionization channel, used for momentum calibration of the time-of-flight spectrometer. (b) is a projection of a small slice from the center of (a). One can clearly see the $3l3l'$ Auger lines in the forward and backward directions and the strong peak associated with the electrons emitted in the forward direction with small velocities relative to the projectile.

be isolated in our experiment by recording electrons in coincidence with C^{5+} and He^{2+} ions. In the corresponding two-dimensional electron-momentum spectra the Auger lines appear as an annular pattern centered on the projectile velocity as seen in Fig. 2(a). In Fig. 2(a) the annular pattern is not uniform, indicating enhanced forward-backward Auger emission. The diameter of the annular region is twice the known Auger electron momentum. Figure 2(b) is a projection of a small slice (around $P_Y=0$) of Fig. 2(a) on the Z -momentum axis where the location of the electrons emitted from the $n=3, n'=3$ states can be clearly identified. The most dominant feature in both Figs. 2(a) and 2(b) is the large broad peak at velocities just above v_p . These electrons are emitted from the projectile with very low energies (≈ 70 meV) and possibly originate from high-lying doubly excited states. A similar peak is not seen in the backwards direction in the frame of the projectile as is seen with the $n=3, n'=3$ Auger lines. We have no physical explanation for the origin of this strange asymmetry, and indeed its origin poses very

intriguing questions, but this is another subject and is not in the scope of this paper. Comparison of our $3l3l'$ spectrum with that of Stolterfoht *et al.* [23] and the calculations of Bhalla *et al.* [24] verifies our computed momentum calibration. The location of $Z=0$ in our electron spectrum was calculated on the assumption that the electric-field axis was perpendicular to the detector surfaces (magnetic-field effects were minimized by the Helmholtz coils). The possibility of small misalignments of the electric field or position of the detectors could be corrected for by using the observed location of the center of the transfer ionization annuli. The center lies at the (Y,Z) position corresponding in velocity space to the projectile velocity, and the known momentum calibration was used to calculate the zero position. The zero position could also be checked by examination of the Z -momentum distributions for the ionization channel. When projecting the two-dimensional spectra on the Z axis for only small P_Y , a small kink appears in the distribution (see Sec. IV), at the velocity of the projectile, corresponding to ECC electrons. The location of $P_Z=0$ in the final momentum spectra was determined with a precision of ± 0.06 a.u. and the momentum scaling better than 5%.

The electron (Y,Z) momentum resolution in our experiment depends on several factors: (1) the initial momentum of the electron, (2) the initial momentum of the recoil ion, and (3) the position resolution of the detectors. The initial electron momentum affects the resolution in the following way. The Z - and Y -positions on the electron detector are related to the initial velocities by $Z=v_z t$ and $Y=v_y t$, respectively, where t is the TOF of the electron. For an electron born at rest, t is about 3.4 nsec, and the spread in t due to different initial X momenta is less than 1 nsec, too small to be measured with our time resolution. Accordingly, the initial X momentum of the electron cannot be determined in our experiment. This unresolved spread in t leads to an uncertainty in the calculation of v_z and v_y . The size of this effect on the Y and Z resolution was determined with the knowledge that the electron momentum distribution is cylindrically symmetric about the Z axis, i.e., the X -momentum distribution is the same as the Y distribution. Using this assumption the Z (Y) momentum uncertainty was calculated to be $0.08 \times p_{Z(Y)}$ full width at half maximum (FWHM) in the worst case of protons on He at $v_p = 2.39$ where the Y -momentum distribution has the largest width. For C^{6+} on He at $v_p = 1.63$ the resolution was calculated to be $0.04 \times p_{Z(Y)}$ FWHM.

The detected position of the recoil ion is assumed to be traceable back to the origin of the ionization event (see Fig. 1). This would be completely true if the initial momentum of the recoil ions were zero. Since the He atoms initially have a room-temperature thermal distribution and the recoil ions get a “kick” from the collision, there is some error in determining the origin of the ionization event, which translates into decreasing the resolution of the EEMD. The momentum given to the recoil ion in the longitudinal direction (Z direction) is about 0.25 a.u. and has a negligible effect on the resolution. Wu [25] measured the transverse recoil ion momentum [$P_{\perp} = (P_x^2 + P_y^2)^{1/2}$] for $O^{8+} + He \rightarrow O^{8+} + He^+ + e^-$ at $v_p = 1.34 - 1.53$ a.u. Assuming that the recoil ion momentum will be similar in our experiment using C^{6+} at similar velocities, we can estimate what the Y -direction momentum distribution will look like and its effect on the EEMD resolution. Estimating the initial X and Y momentum to be

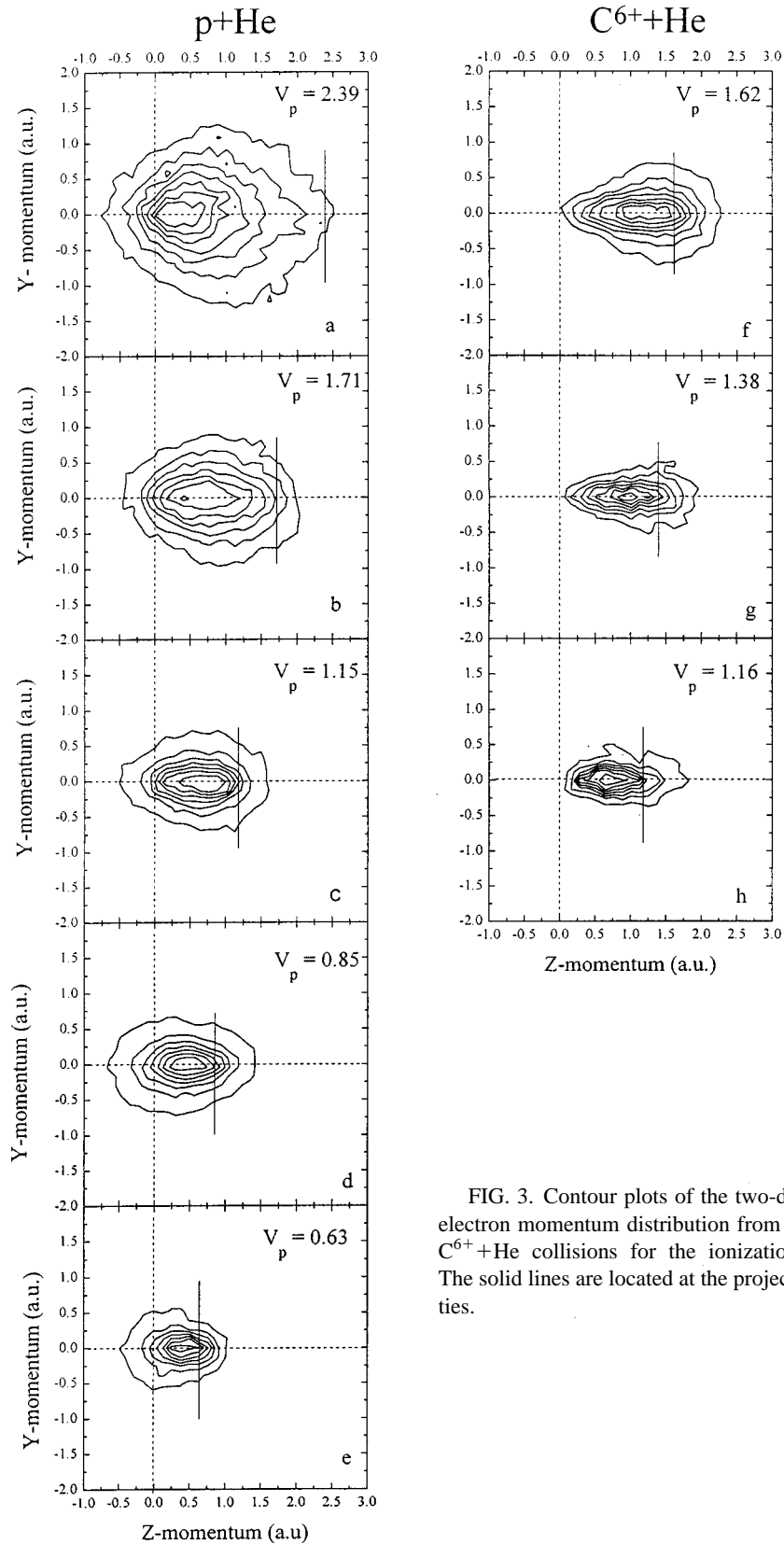


FIG. 3. Contour plots of the two-dimensional electron momentum distribution from $p+\text{He}$ and $\text{C}^{6+}+\text{He}$ collisions for the ionization channel. The solid lines are located at the projectile velocities.

$\pm 3.4 \text{ a.u.}$, the effect from this on the Y -direction resolution is 0.15 a.u. The initial X momentum of the recoil ion has no consequence on the resolution because of the strong electric field in the X direction. For the proton data we know only of

recoil P_{\perp} data at projectile velocities well above [26] ($v_p = 4.47$) and at our lowest velocity [27] ($v_p = 0.63$). Assuming P_{\perp} behaves similarly to that predicted by the Rutherford scattering formula

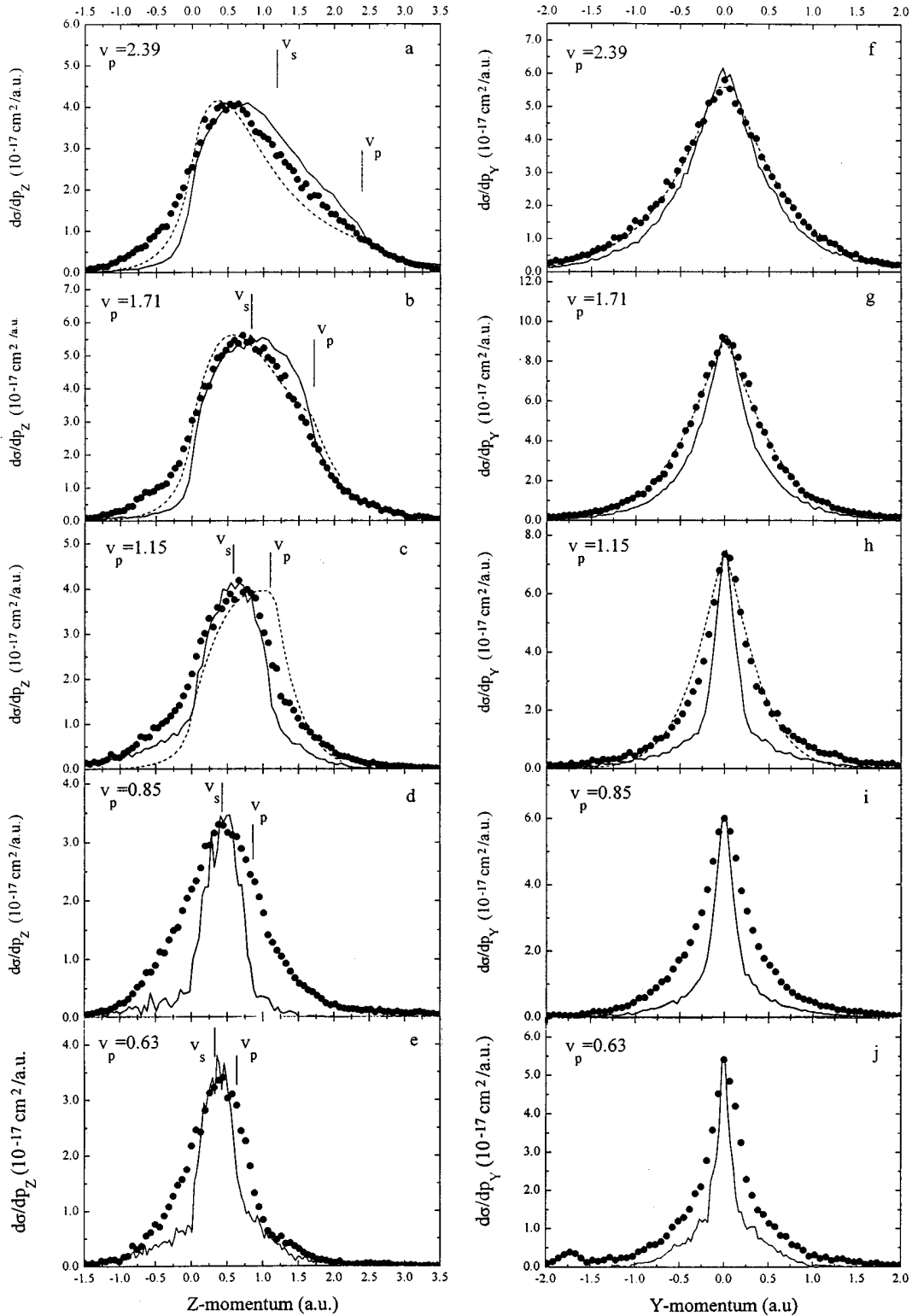


FIG. 4. Z- and Y-electron momentum distributions from the ionization channel, for $p+\text{He}$ collisions for $v_p=2.39, 1.71, 1.15, 0.85,$ and 0.63 a.u. The filled circles are the experimental data, the dashed lines are the CDW-EIS results, and the solid lines are the CTMC results. The short lines annotated by v_s and v_p indicate the position of the saddle-point electron velocity calculated from Eq. (1) and electrons with the projectile velocity, respectively.

$$P_{\perp} = \frac{2q_p q_t}{bv_p},$$

where b is the impact parameter, we estimated a character-

istic width of the recoil Y-momentum distribution to be ± 1.6 a.u. This affects the resolution by 0.07 a.u.

Finally, the position resolution of our recoil and electron detectors is about 0.5 mm, which translates into a momentum

TABLE I. Values by which the CDW-EIS and CTMC present theoretical results were multiplied in the Z and Y directions so that the peaks of the distributions coincided with those of the present experimental results. CDW-EIS calculations were not performed for proton data below 1.15 a.u. (see text), indicated by -. Absolute total cross sections for the CTMC results at the lowest velocities for both the proton and C^{6+} data were not determined and are indicated by * in the table.

Collision velocity (a.u.)	CDW-EIS		CTMC	
	Z	Y	Z	Y
$C^{6+} + He$				
1.63	0.44	0.97	1.52	0.90
1.38	0.45	1.14	0.60	0.60
1.16	0.84	2.35	*	*
$p + He$				
2.39	0.77	0.91	1.12	0.94
1.71	0.94	1	1.61	1.25
1.15	1	1.14	2.27	1.65
0.85	-	-	1.59	2.30
0.63	-	-	*	*

resolution of 0.06 a.u. Adding the different contributions to the resolution, in quadrature, for the proton data yields

$$\Delta P_Z = [(0.08P_z)^2 + 2(0.06)^2]^{1/2},$$

$$\Delta P_Y = [(0.08P_Y)^2 + (0.07)^2 + 2(0.06)^2]^{1/2},$$

and for the C^{6+} data,

$$\Delta P_Z = [(0.04P_z)^2 + 2(0.06)^2]^{1/2},$$

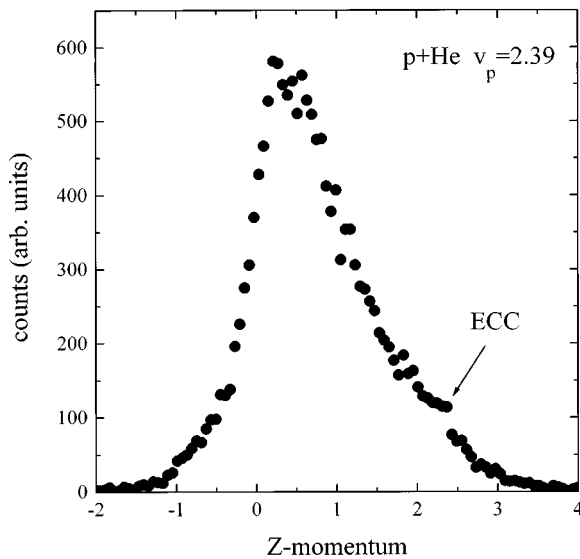


FIG. 5. The same experimental data as displayed in Fig. 4(a) but the projection onto the Z axis is only for small Y momentum ($P_Y \approx \pm 0.18$ a.u.). The kink in the distribution caused by ECC electrons is clearly observed.

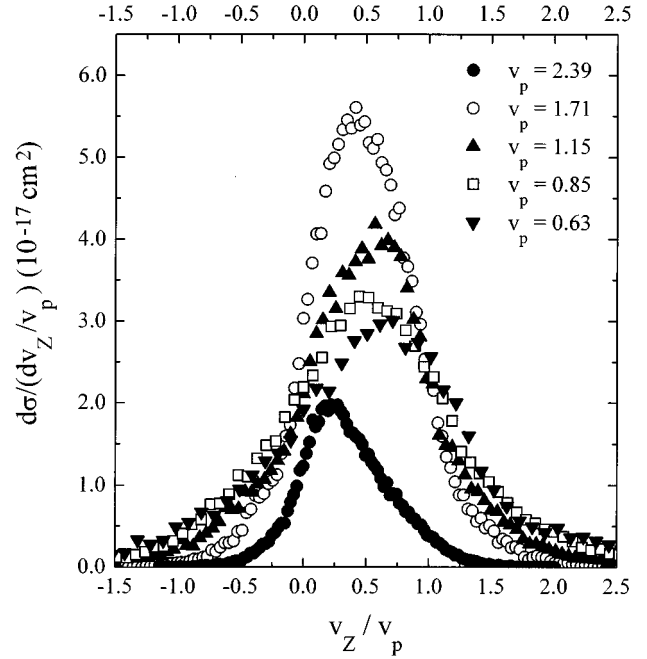


FIG. 6. Plot of the experimental Z electron momentum distributions vs the Z electron velocity over the projectile velocity, for $p+He$ collisions resulting in pure ionization.

$$\Delta P_Y = [(0.04P_Y)^2 + (0.15)^2 + 2(0.06)^2]^{1/2}.$$

III. QUALITATIVE COMPARISON OF PROTON AND C^{6+} RESULTS

Figures 3(a)–3(e) [3(f)–3(h)] are two-dimensional contour plots of the EEMD for the proton (C^{6+}) data. The differences of magnitude between contour lines of individual plots are constant in spacing, but differ between plots due to the differing number of counts in each spectrum. Figure 3 gives a clear picture of the two-dimensional momentum distribution, and the differences between the proton and C^{6+} data become obvious. These two-dimensional representations of the EEMD demonstrate the visual advantages of this technique for electron spectroscopy. The C^{6+} data are clearly narrower than the proton data in the Z and Y directions. Also the C^{6+} data are strongly forward peaked and peak at higher momentum in the Z direction, relative to v_p , than do the proton data for a given v_p . The number of backward ejected electrons ($P_Z < 0$) for the proton data is significant while the C^{6+} data have very few electrons emitted in the backwards direction. The peak shift behavior as a function of v_p is also different. The proton data go from peaking near the target at high-impact velocities to peaking near $v_p/2$ at lower-impact velocities. On the other hand, the C^{6+} projectile data are shifted strongly toward v_p . The narrower and more forward peaked C^{6+} data can be the effect of the much stronger projectile interaction with the ejected electron than is the case with the proton projectile.

IV. RESULTS: $H^+ + He \rightarrow H^+ + He^+ + e^-$

Figures 4(a)–4(e) [4(f)–4(j)] show the projections onto the Z(Y) axes of the proton spectra in Figs. 3(a)–3(e). The

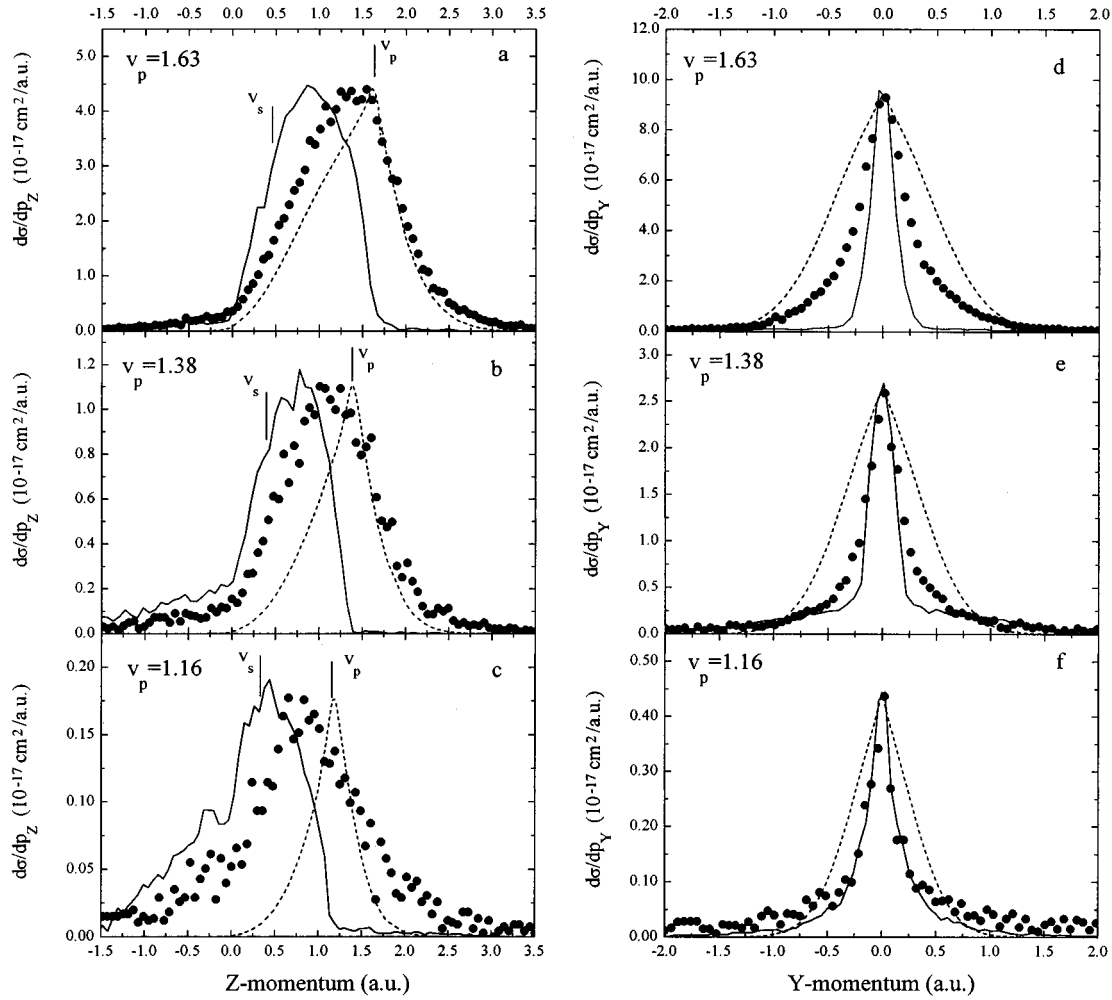


FIG. 7. Z- and Y-electron momentum distributions from the ionization channel, for $C^{6+} + He$ collisions for $v_p = 1.63, 1.38,$ and 1.16 a.u. The filled circles are the experimental data, the dashed lines are the CDW-EIS results, and the solid lines are the CTMC results. The short lines annotated by v_s and v_p indicate the position of the saddle-point electron velocity calculated from Eq. (1) and electrons with the projectile velocity, respectively.

experimental data are compared with the CDW-EIS and CTMC theoretical calculations. The experimental data were integrated and then normalized to the total ionization cross sections [28]. The peak heights of the theoretical results were scaled to coincide with the experimental peak heights so that the momentum-distribution shapes could be easily compared. Table I contains the values the theoretical results were multiplied by. In general, the experimental and theoretical results are in good agreement, except for $v_p = 1.15$ a.u., where the CDW-EIS result is more strongly peaked near the projectile velocity (Z distribution) than is the experiment. Results for the CDW-EIS are not shown below $v_p = 1.15$ a.u. since it is known that the theory is not valid for those low velocities.

The progression of the spectra of Figs. 3 and 4 as the projectile velocity is lowered can be discussed as a continual progression from high- to low-velocity impact ionization mechanisms. Beginning at the highest velocity of 2.39 a.u., for which DI (soft electrons) and ECC (cusp electrons) are still appropriate terms, one can identify the major ionization mechanism as being DI to the target continuum. A small kink in the EEMD exists at v_p that represents capture into

the projectile continuum. This kink is much more noticeable when electrons with only small Y momenta are examined as shown in Fig. 5. Such a spectrum that integrates over all X momenta still emphasizes forward electrons. The kink seen in that spectrum is that seen in the energy-loss spectra of Vajnai *et al.* [29] and corresponds to the cusp peak routinely observed in 0° spectra at high velocities. It is clear that, even at this velocity, this feature represents only a small contribution to the total cross section and would likely be overlooked without emphasis on forward directed electrons. As v_p is reduced, DI electrons can more strongly interact with the Coulomb potential of the outgoing proton; thus the DI electrons can be described as focused and pulled toward the projectile [30]. This shifts the DI electron peak closer to v_p in the longitudinal (Z) direction and narrows the distribution in the Y direction. As v_p is reduced, the ECC contribution appears to grow in relative importance, but the overlap of these ECC electrons with the DI peak becomes so strong that it is no longer possible to describe these as different features in the spectrum. The two features in the spectra coalesce into a single peak that seems to settle at approximately the velocity

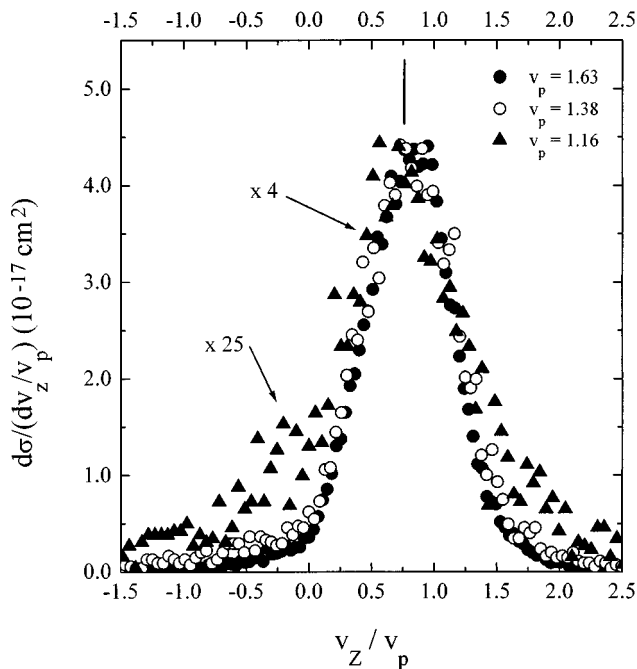


FIG. 8. Plot of the experimental Z-electron momentum distributions vs the Z-electron velocity over the projectile velocity for $C^{6+} + He$ collisions resulting in pure ionization.

of the saddle of two singly charged ionic cores. Whether this result by itself constitutes evidence for the dominance of the T process is not immediately claimed, but the data certainly seem qualitatively consistent with the physical picture of saddle-point electrons. The evolution of the longitudinal momentum spectrum from the target centered toward the saddle is emphasized in Fig. 6, where the data are plotted versus v_z/v_p , thereby removing the influence of the overall scale factor v_p from the appearance. This evolution of the spectrum is qualitatively described by both the CDW-EIS and CTMC calculations, although the former seems to overestimate the importance of the projectile-electron interaction at $v_p = 1.15$ a.u.

The relative narrowing of the spectrum in the transverse (Y) direction is also rather well described by both calculations. We note that, because of the rather complicated dependence of the resolution function on the electron momenta, we have not tried to fold the theoretical spectra into the experimental resolution function. Such a folding would be expected to have only a small effect on most of the spectra, but for the very narrow transverse distributions at $v = 0.85$ a.u. and below such a folding would improve the agreement between the CTMC and experimental transverse spectra. The transverse spectra evolve from nearly equal longitudinal width at 2.39 a.u. to sharply centered on the beam axis at low velocities. Such a behavior could be ascribed within the saddle-point terminology as due to an adiabatic transverse cooling of the electrons as the transverse harmonic potential well seen by these electrons gradually dissolves as the ion cores recede from each other.

V. RESULTS: $C^{6+} + He \rightarrow C^{6+} + He + e^-$

Figures 7(a)–7(c) [7(d)–7(f)], show the $Z(Y)$ projections of the C^{6+} projectile data in Figs. 3(f) and 3(g). The C^{6+}

experimental results were normalized to the total cross sections [4] and the theoretical results were scaled in the same way the proton data were (see Sec. III and Table I). The experimental EEMD for the C^{6+} data are substantially different from those of the proton data.

We note that while the velocity range covered by the proton data go from below to above the velocity-matching maximum in the total cross section, the C^{6+} data all lie at velocities far below the corresponding maximum, and thus should be viewed as representing only the low-velocity region. The longitudinal spectra are resolutely centered at a velocity of about $3/4 v_p$ in all spectra. This characteristic is more clearly shown in Fig. 8, which shows these spectra plotted versus v_z/v_p . There is no evidence of any feature in the spectra at the location of the saddle, which, for a C^{6+} core receding from a He^+ core, would be located at $v_z = 0.29v_p$. On its surface, it would appear that the data do not support the most naive picture of ionization through the saddle-point or T -process mechanism. On the other hand, the maximum in the spectra of Figs. 7 and 8 does appear to be near the velocity of the center of mass of the system, $v_z = 0.76v_p$. It is suggested by Bárány and Ovchinnikov [7] that the S process should produce continuum electrons centered near this velocity for highly charged projectiles. (We have unpublished data for other systems that indicate that the near exact coincidence of this maximum with the center-of-mass velocity is somewhat accidental.) The experimental result might be interpreted as evidence for the importance of the S process as an ionization mechanism. Our results appear to be contrary to the calculations of Bárány and Ovchinnikov [7], who predict that the S and T processes are important in ionization of hydrogen by highly charged ions in the energy range we have studied. However, we point out that no quantitative evaluation of the expected spectrum for either the S or T process has ever been made for a highly charged projectile, and that only qualitative predictions are presently available. The data seem to state that the strong C^{6+} potential insists on carrying not only captured but also continuum electrons with it as it departs.

To some extent this behavior is predicted by the theoretical calculations. In particular, the CDW-EIS predicts that at all three velocities studied here the EEMD are strongly peaked at v_p in the Z direction. However, this calculation gives a much too sharply peaked longitudinal distribution, especially for the lower two values of v_p , and seems to overemphasize the role of the projectile potential. The CTMC result predicts that hardly any electrons are ejected with velocities of v_p , in disagreement with the experimental results. Both the CDW-EIS and the CTMC reproduce the relatively narrow transverse momentum distributions, with the CTMC doing the better job. The physical origin of this behavior may again be attributed to transverse cooling of the electrons near the saddle, which could be an operative mechanism, even if the final electron longitudinal velocity is not at the saddle-point velocity. It should be noted that the close-coupling calculations of Wang *et al.* [31] provided correct results for total ionization cross sections of He by C^{6+} in this velocity range, but that these calculations cannot yet be formulated in such a way as to provide reliable EEMDs.

VI. CONCLUSIONS AND SUMMARY

We have presented ejected electron-momentum spectra, or EEMDs, for ionization of He by slow protons and bare carbon nuclei. For the proton case the longitudinal momentum spectra at the highest projectile velocities are dominated by soft electrons in the target continuum, with a small contribution of cusp electrons. These two features coalesce as the projectile velocity is lowered, and finally center at a Z velocity near that of the saddle point. The transverse momentum distributions at the lowest velocities are much narrower than are the longitudinal distributions. The CDW-EIS method gives an excellent description of the EEMDs for the higher velocities, but are less successful as v_p is lowered. The CTMC is rather successful in describing the main features of the EEMDs at all velocities. For the C^{6+} data, no evidence for any feature that can be identified as saddle-point electron emission is seen. The longitudinal momentum distributions are centered more nearly on the velocity of the center-of-mass of the system than on the saddle-point velocity. If this result were to be taken literally as evidence that

the T process is not dominant, it would appear to be at odds with the agreement of the total ionization cross sections by slow bare nuclei with a scaling law suggested by Wu *et al.* [17]. The origin of this scaling law was suggested by its similarity to one for the T process. However, in the absence of explicit calculations for either total cross sections or EEMDs for either S or T processes for highly charged projectiles on He, no conclusive interpretation of the data in terms of these two mechanisms can be drawn. Neither the CDW-EIS nor the CTMC predictions are as successful for this case as for proton projectiles. We await further theoretical activity in this area.

ACKNOWLEDGMENTS

We would like to acknowledge C. Bhalla and R. Dorner for enlightening conversations. This work was supported by the Division of Chemical Sciences, Office of Basic Energy Sciences, Office of Energy Research, U.S. Department of Energy. M.P. acknowledges support from the Netherlands Organization for Scientific Research (NWO).

-
- [1] M. E. Rudd, Y.-K. Kim, D. H. Madison, and T. J. Gay, *Rev. Mod. Phys.* **64**, 441 (1992).
- [2] R. Shakeshaft, *Phys. Rev. A* **18**, 1930 (1978).
- [3] T. J. Park, J. E. Aldag, J. M. George, J. L. Peacher, and J. H. McGuire, *Phys. Rev. A* **15**, 508 (1977).
- [4] R. E. Olson, *Phys. Rev. A* **27**, 1871 (1983).
- [5] R. E. Olson, T. J. Gay, H. G. Berry, E. B. Hale, and V. D. Irby, *Phys. Rev. Lett.* **59**, 36 (1987).
- [6] T. G. Winter and C. D. Lin, *Phys. Rev. A* **29**, 3071 (1984).
- [7] A. Bárány and S. Ovchinnikov, *Phys. Scr.* **T46**, 243 (1993).
- [8] S. Y. Ovchinnikov and E. A. Solev'ev, *Zh. Eksp. Teor. Fiz.* **90**, 921 (1986) [*Sov. Phys. JETP* **63**, 538 (1986)].
- [9] M. Pieksma and S. Y. Ovchinnikov, *J. Phys. B* **24**, 2699 (1991).
- [10] S. Yu. Ovchinnikov and J. H. Macek, *Phys. Rev. Lett.* **75**, 2474 (1995).
- [11] V. D. Irby, T. J. Gay, J. Wm. Edwards, E. B. Hale, M. L. Mckenzie, and R. E. Olson, *Phys. Rev. A* **37**, 3612 (1988); T. J. Gay, M. W. Gealy, and M. E. Rudd, *J. Phys. B* **23**, L823 (1990).
- [12] R. D. Dubois, *Phys. Rev. A* **48**, 1123 (1993).
- [13] V. D. Irby, S. Datz, P. F. Dittner, N. L. Jones, H. F. Krause, and C. R. Vane, *Phys. Rev. A* **47**, 2957 (1993).
- [14] R. D. Dubois, *Phys. Rev. A* **50**, 364 (1994).
- [15] W. Meckbach, S. Suarez, P. Focke, and G. Bernardi, *J. Phys. B* **24**, 3763 (1991).
- [16] M. Pieksma, S. Y. Ovchinnikov, J. van Eck, W. B. Westerveld, and A. Niehaus, *Phys. Rev. Lett.* **73**, 46 (1994).
- [17] W. Wu, C. L. Cocke, J. P. Giese, F. Melchert, M. L. A. Raphaelian, and M. Stockli, *Phys. Rev. Lett.* **75**, 1054 (1995).
- [18] D. S. F. Crothers and J. F. McCann, *J. Phys. B* **16**, 3239 (1983).
- [19] P. D. Fainstein, V. H. Ponce, and R. D. Rivarola, *J. Phys. B* **24**, 3091 (1991).
- [20] R. E. Olson and A. Salop, *Phys. Rev. A* **16**, 531 (1977).
- [21] Y. D. Wang, V. D. Rodríguez, C. D. Lin, C. L. Cocke, S. D. Kravis, M. Abdallah, and R. Dörner, *Phys. Rev. A* **53**, 3278 (1996).
- [22] M. P. Stockli, R. M. Ali, C. L. Cocke, M. L. A. Raphaelian, P. Richard, and T. N. Tipping, *Rev. Sci. Instrum.* **63**, 2822 (1991).
- [23] N. Stolterfoht, K. Sommer, J. K. Swenson, C. C. Havener, and F. W. Meyer, *Phys. Rev. A* **42**, 5396 (1990).
- [24] C. P. Bhalla, S. R. Grabbe, and A. K. Bhatia, *Phys. Rev. A* **52**, 2109 (1995).
- [25] W. Wu, Ph. D. dissertation, Kansas State University (1994).
- [26] R. Dörner, V. Mergel, Liu Zhaoyuan, J. Ullrich, L. Spielberger, R. E. Olson, and H. Schmidt-Böcking, *J. Phys. B* **28**, 435 (1995).
- [27] M. E. Rudd *et al.*, *At. Data Nucl. Data Tables* **18**, 413 (1976).
- [28] T. Vajnai, A. D. Gaus, J. A. Brand, W. Htwe, D. H. Madison, R. E. Olson, J. L. Peacher, and M. Schulz, *Phys. Rev. A* **74**, 3588 (1995).
- [29] O. Jagutzki, R. Koch, A. Skutlartz, C. Kelbch, and H. Schmidt-Böcking, *J. Phys. B* **24**, 993 (1991).
- [30] Y. D. Wang, C. D. Lin, N. Toshima, and Z. Chen, *Phys. Rev. A* **52**, 2852 (1995).